Direct observation of the fayalite slag formation behaviour from large SiO_2 grains

Y. Goto[1,2], *S. Kawanishi*[3], *S. Natsui*[4], *J. Takahashi*[5], *and H. Nogami*[6]

1. Manager, Sumitomo Metal Mining Co., Ltd., Tokyo, 105-8716. Email: yuko.goto.r4@smm-g.com
2. PhD student, Tohoku University, Miyagi, 980-8577. Email: goto.yuko.t7@dc.tohoku.ac.jp
3. Associate Professor, Kyoto University, Kyoto, 606-8501. Email: kawanishi.sakiko.6h@kyoto-u.ac.jp
4. Associate Professor, Tohoku University, Miyagi, 980-8577. Email: natsui@tohoku.ac.jp
5. Chief Staff, Research & Development, Sumitomo Metal Mining Co., Ltd., Tokyo, 105-8716. Email: junichi.takahashi.e4@smm-g.com
6. Professor, Tohoku University, Miyagi, 980-8577. Email: nogami@tohoku.ac.jp

Keywords: flash furnace, fayalite slag, silica flux, direct observation, interfacial reaction

ABSTRACT

The demand for copper increases yearly, and further improvements in copper smelting efficiency using flash furnaces are required. This study was conducted to understand and promote the interfacial reaction associated with the collision of silica flux and iron oxide particles, i.e. the formation reaction of fayalite slag, in the reaction shaft of the flash furnace. High-temperature microscopy was used to observe the reaction behaviour of a 2 mm granular SiO_2 reagent in contact with micrometre-order-sized FeO reagents in situ. When the amount of FeO was lower than the stoichiometric amount with SiO_2, the molten slag formed at the interface between FeO and SiO_2 diffused into the SiO_2 particle before dissolving the remaining FeO particles. It did not contribute to the subsequent reaction, and despite having the lowest amount of FeO among the samples in this study, many unreacted FeO particles remained on the surface of the samples after testing. On the other hand, under conditions with high FeO content and close to the eutectic composition of the FeO-SiO_2 system, a liquid phase formed from low temperatures, gradually increasing in volume and eventually completely dissolving the 2 mm SiO_2 grain. These results indicate that the early-stage slag is essential in increasing the interfacial area between FeO and SiO_2 and facilitating the supply of FeO to SiO_2. In other words, the FeO/SiO_2 determines the amount of liquid phase and significantly influences the subsequent interfacial reaction rate between FeO and SiO_2. Therefore, the local FeO/SiO_2 of the particles falling down the reaction shaft should also be optimised to ensure early slag formation. Meanwhile, the time required for 2 mm SiO_2 to complete the reaction for the temperature history employed in this study was significantly longer than the particle residence time in the reaction shaft. Further detailed investigation of the effects of silica flux particle size, composition, and reaction temperature on the reaction time will help find the conditions under which the reaction of silica flux can be completed in the reaction shaft. These kinetic approaches could contribute to future innovations in the copper smelting process using flash furnaces.

INTRODUCTION

Copper is mainly used in electrical and telecommunications infrastructure and small equipment. The demand for copper is increasing year by year due to the development of the global economy and the drive towards electrification (ICSG (2023)). With a new specific target of 'triple renewable energy by 2030' included in COP28 (2023), demand for copper is expected to grow further. In copper smelting, there is a need for technological innovations to increase smelting efficiency further.

Figure 1 shows a schematic diagram of the most common copper smelting furnace, the Outokumpu-type flash furnace (Kojo et al. (2000); Kojo et al. (2015); ICSG (2023)). The copper concentrate consists of copper and iron sulphides, is injected through the concentrate burner with oxygen-enriched air and silica flux, and reacts in the reaction shaft in the flash furnace. Sulfur in the concentrate is oxidised to SO_2 by oxygen-enriched air and separated into the gas phase. Iron in the concentrate is oxidised to iron oxide (FeO*x*), which further reacts with SiO_2 to form fayalite slag (FeO*x*-SiO_2). Copper in the concentrate is concentrated in copper matte (Cu_2S-FeS) by separating

S and Fe. Copper matte is recovered from the slag by specific gravity separation at the settler, tapped through the matte holes and sent to the converter. The viscosity of the molten slag and the presence of a spinel, e.g. Fe_3O_4, significantly affect the matte's settling rate, which in turn significantly affects the matte yield (De Wilde et al. (2016)). For this reason, many studies on slag chemistry based on the equilibrium theory have been conducted, e.g. by Muan (1955); Yazawa (1979); Vartiainen (1982); Taskinen et al. (2005); Jak et al. (2007); Shishin et al. (2018). Although the reaction shaft is the flash furnace's main reaction field, few studies still focus on slag formation behaviour in the reaction shaft. To the authors' knowledge, there are studies carried out by Takebe et al. (2019); Nishioka et al. (2022); Natsui et al. (2023), but the discussions based on kinetics are insufficient.

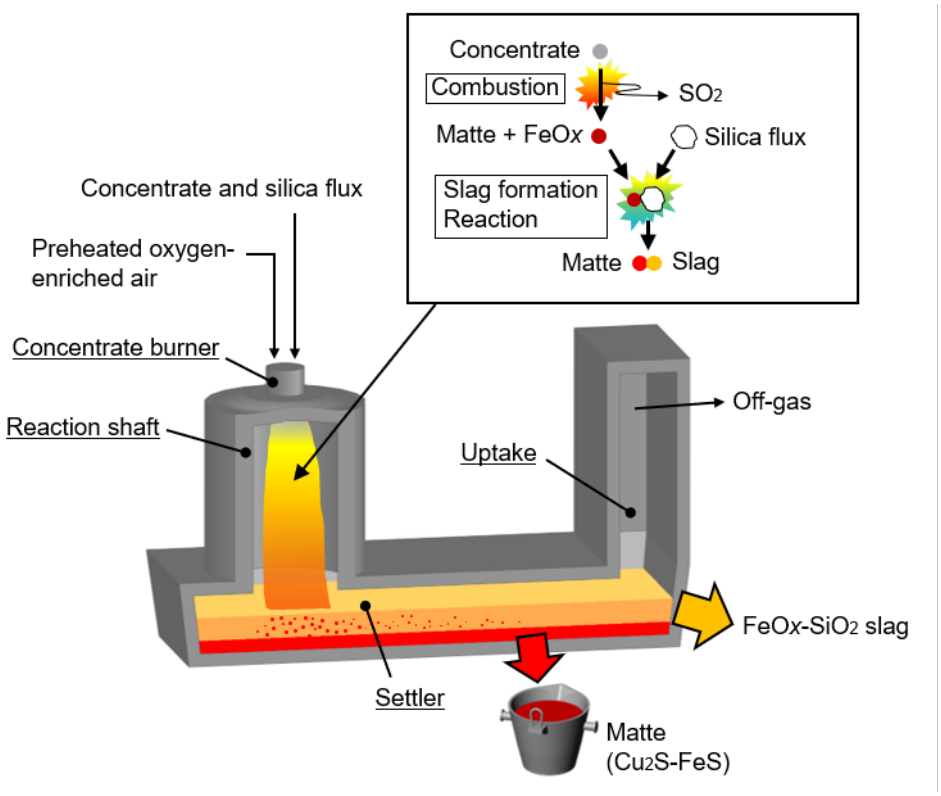

FIG 1 – Outokumpu type flash furnace and image of reaction mechanism in reaction shaft.

SiO_2, a raw material of fayalite slag, is supplied additionally to the flash furnace as silica flux. Silica flux can contribute to slag formation only if it is heated up to the reaction temperature and if it comes into contact with the iron oxides produced by the oxidation of the concentrate (Kemori et al. (1989); Goto et al. (2024)). The silica fluxes, however, are unlikely to be heated quickly because their size is usually larger than that of the concentrates (Ahokainen and Jokilaakso (1998); Taskinen and Jokilaakso (2021)). Furthermore, it is known that the residence time of the particles in the reaction shaft is extremely short, around 1 second or 2-3 seconds at most (Solnordal et al. (2006); Taskinen and Jokilaakso (2021); Nirmal Kumar et al. (2022)). A detailed understanding of the $FeOx$-SiO_2 interfacial reactions and the SiO_2 heating process is essential to complete the slag formation reaction within this short residence time.

To understand the formation behaviour of fayalite slag following the collision of silica flux and iron oxide particles in the flash furnace reaction shaft, this study observed the reaction behaviour of SiO_2 reagents in contact with FeO reagents in situ using high-temperature microscopy (Goto et al. (2024)). Since the silica flux fed to the flash furnace generally has a larger grain size than the concentrate, this study used a 2 mm granular SiO_2 reagent and reacted with a micrometre-order-sized FeO reagent. The formation of fayalite slag from granular SiO_2 was directly observed, and the effect of the FeO/SiO_2 ratio on fayalite slag formation behaviour was visualised.

EXPERIMENTAL WORK

Experimental apparatus

A schematic diagram of the high-temperature microscopy system used in this study is shown in Figure 2. The system consists of an infrared gold image furnace (SVF18SP, Yonekura MFG., Japan) for heating the sample, a microscope with a CMOS digital camera for observing the interface in the sample, a light source and an oxygen partial pressure controller (SiOC-200C, STLab Co., Ltd., Japan). The infrared gold image furnace has an oval-shaped chamber to which a dish-shaped sample holder with a thermocouple is attached at the upper focal point. The sample is heated by focusing infrared radiation. An observation window is mounted on the top of the chamber to observe the heated sample from outside the furnace. A microscope is installed above the observation window, and white light from the light source is irradiated through the microscope's objective lens onto the sample to obtain a bright-field image. A digital camera electronically records the variation of the sample appearance during the reaction. The oxygen partial pressure controller was used to control the oxygen partial pressure of the reaction atmosphere.

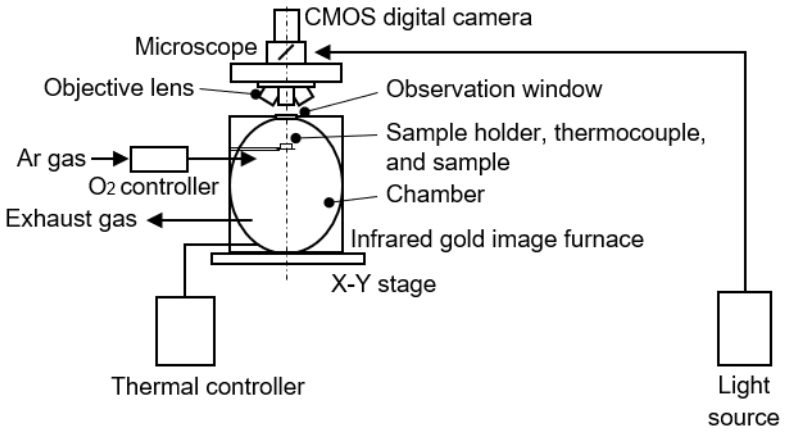

FIG 2 – Schematic diagram of the experimental apparatus.

Experimental procedures

The platinum pan (inner diameter 4.8 mm, depth 2.6 mm) with the sample was placed on the sample holder, and the furnace was sealed. The furnace was depressurised to 5 x 10^{-2} Pa or less using an unshown vacuum pump. The gas in the furnace was then replaced by Ar gas with an adjusted oxygen

partial pressure. The furnace was then heated while the temperature was measured using thermocouples. The melting behaviour of the samples was observed with a microscope through an observation window and an optical filter and recorded electronically using a CMOS digital camera. The image resolution was 960 x 600, and the frame rate was 30 fps.

Sample

In this study, FeO powder reagent (99.5 % purity, Kojundo Chemical Laboratory Co., Ltd., Japan) and cylindrical granular SiO_2 reagent with a diameter of 2 mm and a height of 2 mm (99.99 % purity, Kojundo Chemical Laboratory Co., Ltd., Japan) were used to prepare three different samples. The appearances of the samples before heating are shown in Figure 3. Each sample was prepared by placing FeO reagent on a single SiO_2 grain in a platinum pan, differing only in the amount of FeO reagent. Sample 1 was prepared by putting FeO reagent on a single SiO_2 grain with a molar ratio of FeO : SiO_2 = 2 : 1 (Figure 3a). Sample 2 was prepared by placing a considerably smaller amount of FeO than the stoichiometric ratio on top of the SiO_2 grain as a small pile. Sample 3 was prepared by dispersing an even smaller amount of FeO than in Sample 2 on SiO_2 grain (Figure 3b). Samples 2 and 3 were prepared on the same platinum pan and heated simultaneously.

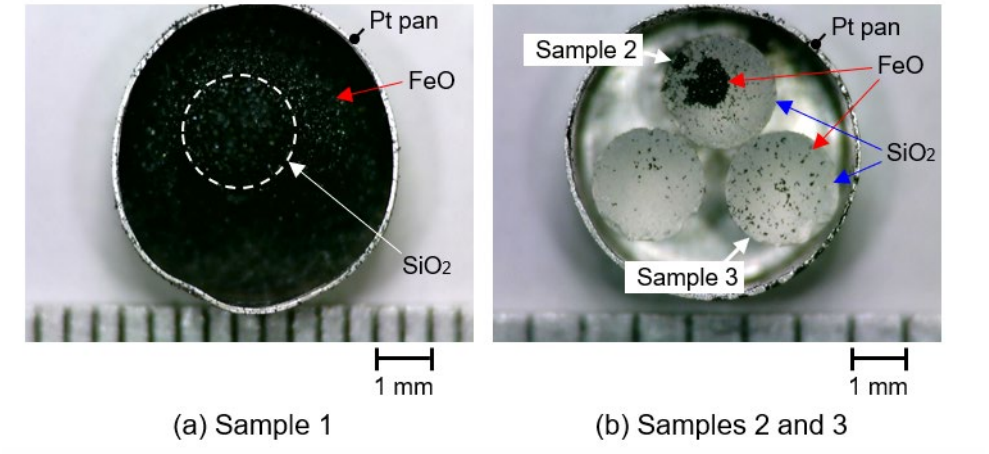

FIG 3 – Samples used in this study.

Experimental conditions

Ar gas of 99.999% purity with a controlled oxygen partial pressure of around 10^{-9} atm was supplied at 200 cm^3/min. The furnace temperature was increased to a maximum of 1673 K, then held at 1673 K for 60 seconds before being lowered in the tests using Sample 1. In the tests using Samples 2 and 3, the furnace temperature was raised to a maximum of 1573 K and immediately lowered. The rate of temperature increase was 200 K/min from room temperature to 1273 K and 50 K/min from 1273 K to the maximum temperature for all samples.

The sample temperature was calibrated by the melting point of copper. The preliminary test of heating metallic copper on an alumina pan was conducted. The furnace temperature measured by the thermocouple at which the metallic copper began to melt was 5 K above the melting point of the

copper. The following sections illustrate the results using sample temperatures corrected 5 K lower than the furnace temperature.

RESULTS AND DISCUSSION

Reaction behaviour of Sample 1

The morphological changes of Sample 1 ($FeO/SiO_2 = 2$) during heating up to 1668 K are shown in Figure 4. The elapsed time after the sample temperature reached 1268 K and the sample temperature are shown in the figure. At 1268 K (Figure 4a), the outline of the SiO_2 grain under the FeO can be seen. At 1413 K (Figure 4b), the outline of the SiO_2 grain is more clearly visible than in Figure 4a due to the furnace luminescence. Subsequently, the formation of a liquid phase at once around 1418 K (Figure 4c) can be seen on the SiO_2 grain. At 1423 K (Figure 4d), the SiO_2 grain starts tilting, suggesting that the reaction progresses at the bottom of the SiO_2 grain. At 1428 K (Figure 4e), the amount of the liquid phase further increases, and the FeO reagent, which appeared to be in a semi-molten state at the bottom of the Pt pan, started to deform as it peeled off from the Pt pan. The reaction progresses further in Figures 4f and 4g, and the SiO_2 grain tilts significantly. In Figure 4h, the SiO_2 grain is considerably soaked in the $FeO\text{-}SiO_2$ slag. Subsequently, as heating continues, the SiO_2 gradually becomes smaller, as shown in Figure 4i and Figure 4j, and at 1668 K (Figure 4k), the SiO_2 grain is almost invisible. The sample was then held at 1668 K for 60 seconds, but no significant change in the appearance of the molten sample was observed (Figure 4l). The time from the liquid phase formation (Figure 4c) to the completion of the reaction (Figure 4k) was 306 seconds. This is about two orders of magnitude longer than the typical residence time in the reaction shaft of a flash furnace.

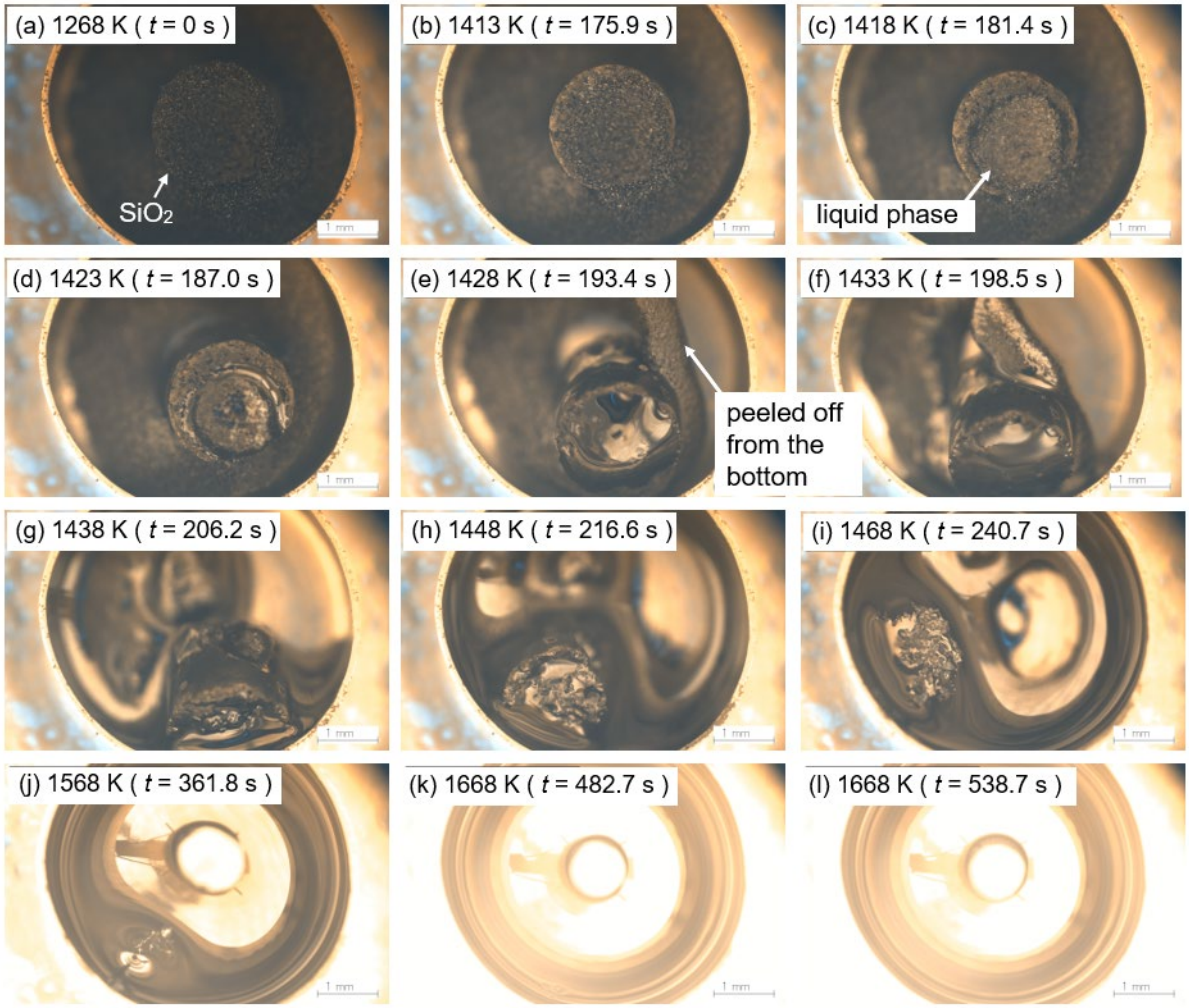

FIG 4 – The morphological change of Sample 1 during heating.

After the test, the sample was cut together with the Pt pan, and an Electron Probe microanalysis (EPMA) of the vertical cross-section was performed. Figure 5 shows the elemental mapping of the cross-section of Sample 1 after the test. A material composed of Fe, Si, and O can be seen in the corner of the platinum pan. The distribution of Fe, Si and O are uniform, and the surface shape of the material is smooth. These results suggest that all the FeO and SiO_2 react and form a uniform melt, the FeO-SiO_2 slag.

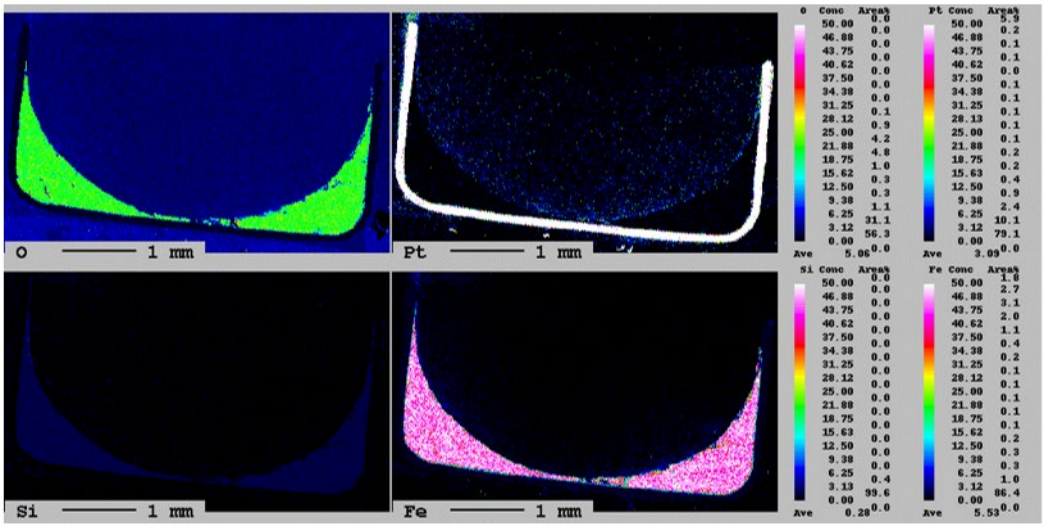

FIG 5 – EPMA image of a cross-section of sample 1 after the test.

Reaction behaviour of Samples 2 and 3

The reaction behaviour of samples with less amount of FeO was observed. Sample 2 is the sample with less than stoichiometric FeO placed as a pile on the SiO_2 grain, and Sample 3 is the sample with even less FeO sprinkled to disperse on the SiO_2 grain. They were placed on the same Pt pan and heated simultaneously to check the effect of the amount of FeO. Figure 6 shows the morphological change of Samples 2 and 3 during heating. Sample 2 is shown in the top right, and Sample 3 in the bottom left. The elapsed time after the sample temperature reached 1268 K and the corresponding temperature are shown in the figure. At 1268 K (Figure 6a) and 1368 K (Figure 6b), angular FeO particles are visible on top of granular SiO_2 in Samples 2 and 3, suggesting that FeO exists in solid. At 1443 K (Figure 6c), some stains appeared near the FeO particles on the top surface of the SiO_2 grain in Sample 2, and at 1448 K (Figure 6d), the liquid phase became visible in the FeO reagent-rich areas. After that, the liquid phase quickly spread throughout the SiO_2 at 1451 K (Figure 6e). The liquid phase was absorbed by the SiO_2 grain at 1453 K (Figure 6f) and was almost invisible in Sample 2 by 1503 K (Figure 6g). Sample 3, on the other hand, showed no significant change in the appearance of FeO until 1503 K (Figure 6g). Further heating up to 1518 K (Figure 6h) resulted in several black stains spreading over Sample 3 at once. Subsequently, heating was continued up to 1568 K (Figure 6i), but no significant change in the sample appearance was observed for both Samples 2 and 3. In Samples 2 and 3, some particles remained in the central part of the stains on the SiO_2 grain surface.

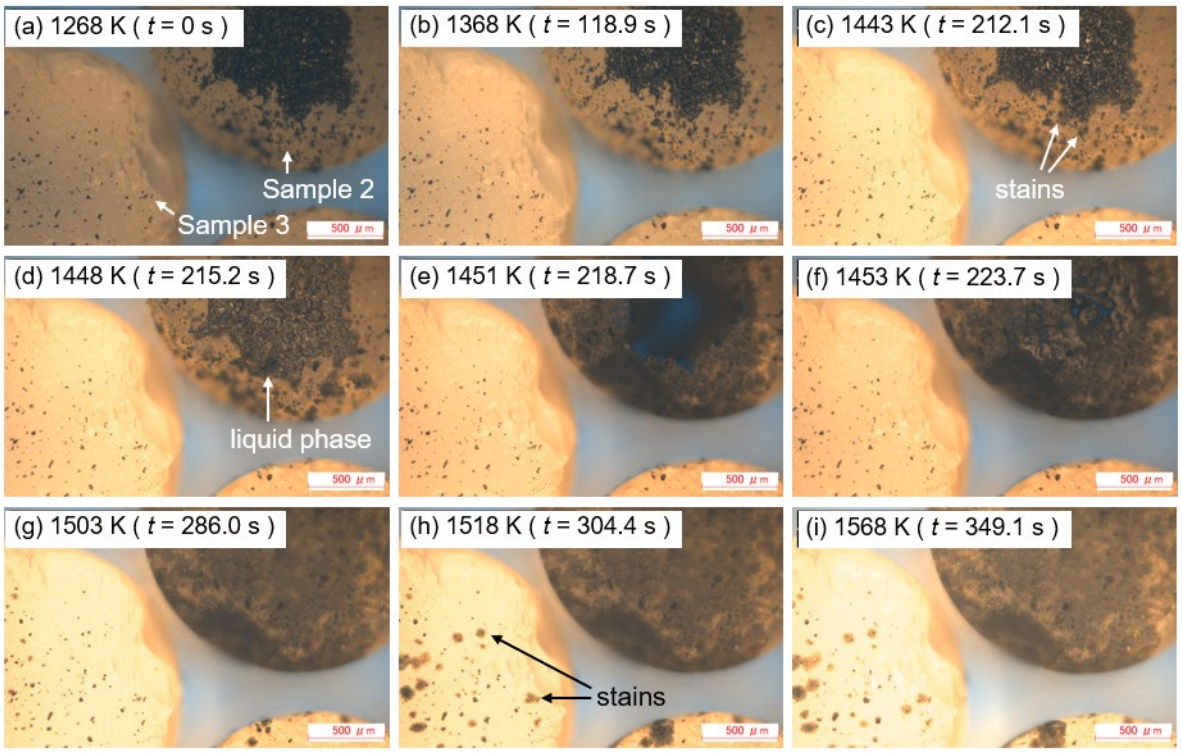

FIG 6 – The morphological change of Samples 2 and 3 during heating.

After the experiment, the surface of the samples was observed. The appearances of the post-test samples are shown in Figure 7. Figures 7a and 7b show the top surface of Samples 2 and 3, respectively. As in the observation image during heating shown in Figure 6, the stains produced by the reaction and several residual particles in the centre of the stains can be seen. In Sample 2, shown in Figure 7a, several stains were linked together to form a single mass. In the middle of the sample, where a large amount of liquid phase was generated, residual particles were hardly visible. On the other hand, in the areas where FeO was dispersed in Samples 2 and 3, the stains were dispersed, and residual particles could be seen in most stains.

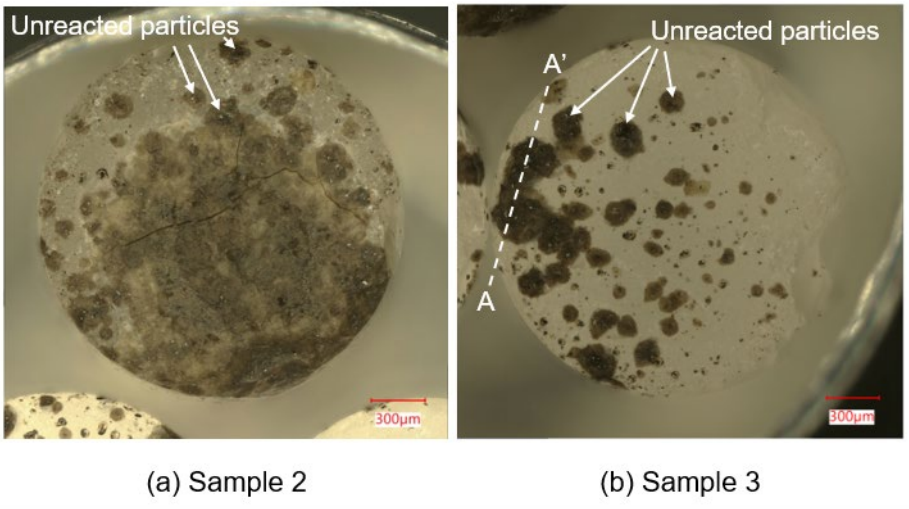

FIG 7 – Photos of Samples 2 and 3 after the experiment.

After the surface observation, Sample 3 was cut, and a cross-section was observed by SEM (Scanning Electron Microscope). Figure 8 shows the SEM image of the cross-section A-A' of Sample 3 in Figure 7b. In Figure 8, white granular material can be seen on the bulk material. Under the white granule, the bulk material is cracked. The EDS (Energy Dispersive X-ray Spectroscopy) analysis shows that these are FeO particle, FeO-SiO_2 and SiO_2, respectively.

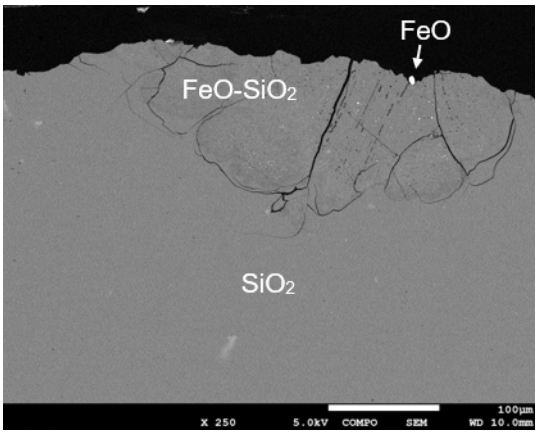

FIG 8 – SEM image of a cross-section of Sample 3 after the test.

Discussion

Table 1 summarises the test results of this study. Figure 9 shows the phase diagram of the FeO-SiO_2 system at p_{O2} = 10^{-9} atm calculated by FactSage 8.3 (Bale et al. 2009) with the line corresponding to the overall composition of Sample 1 (FeO/SiO_2 = 2). Sample 1, with FeO/SiO_2 close to the stoichiometric ratio, had the lowest liquid formation temperature among the samples in this study. No unreacted FeO was identified in the post-test sample, and the entire sample was in a completely liquid phase. This is because the overall composition of the sample was close to the eutectic composition, which allowed the liquid phase to form at low temperatures. The liquid phase further dissolved unreacted FeO and increased the volume. As a result, good contact between FeO and SiO_2 through the liquid phase was achieved. The FeO continued to be supplied to the unreacted bulk SiO_2 as there was sufficient FeO. Coexistence with FeO lowered the melting point of the SiO_2 interface and resulted in the dissolution of all of the SiO_2. On the other hand, in Sample 3, where the FeO was tiny relative to SiO_2, the temperature at which the liquid phase could be seen was 100 K higher than in Sample 1. Although Sample 3 had the lowest amount of FeO, many unreacted FeO particles remained on the sample's surface after the test. This is due to the few FeO particles, which resulted in a smaller contact interface area with SiO_2, delaying the progress of the reaction. Furthermore, the produced slag diffused into the SiO_2 before dissolving the remaining FeO particles. The composition of the SiO_2 inside was on the SiO_2-rich side of the eutectic point on the phase diagram, resulting in a melting point higher than the test temperature reported here. This prevented the subsequent liquid phase formation and the complete dissolution of FeO.

TABLE 1 – Comparison of reaction results for Samples 1 – 3.

		Sample 1	Sample 2	Sample 3
Experimental conditions	FeO/SiO_2	2	Smaller than 2	Extremely small
	Max furnace temperature	1673 K, 60-second hold	1573 K, No hold	
Results	Temperature of liquid phase formation observed	1418 K	1448 K	1518 K
	The degree of reaction of FeO	All reacted	Partially remaining in areas with sparse FeO	Partially remaining

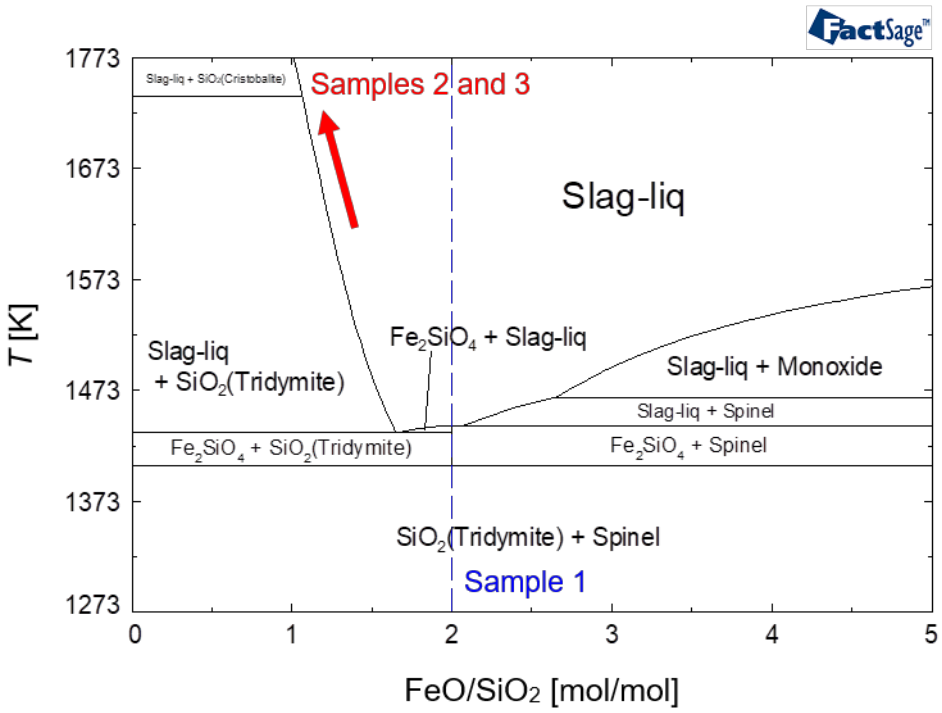

FIG 9 – FeO-SiO_2 phase diagram of p_{O2} = 10^{-9} atm calculated by FactSage 8.3.

To further improve the smelting efficiency of flash furnaces, it will be necessary to promote the slag formation reactions not only in the settler but also in the reaction shaft. This study shows that the reaction hardly proceeds when there is an excess of SiO_2 relative to FeO, even with small amounts of FeO. If the ratio of FeO to SiO_2 is close to the stoichiometric ratio, the reaction is accelerated because a liquid phase formed from low temperatures forms new reaction interfaces. In flash furnace operations, the raw material composition is usually controlled so that the FeO/SiO_2 ratio in the settler slag reaches the desired value, considering slag flowability. This study suggests that the local FeO/SiO_2 ratio in the reaction shaft should also be optimised to promote the formation of fayalite slag.

2-mm-size SiO_2 grain took 306 seconds to dissolve, even in Sample 1, which had the best reactivity among the test conditions in this study. This is considerably longer than the residence time in the reaction shaft. This means that if 2 mm pure SiO_2 were to be fed into the reaction shaft and the temperature history of this study, the slag formation reaction would not be complete in the residence time of the reaction shaft. Of course, a 2 mm feed is quite large in a flash furnace. In addition, the actual temperature history of the silica flux may be higher than the one in this study because there is a local high-temperature field in the reaction shaft (Hahn and Sohn (1990); White et al. (2015)). Future tests should provide a more detailed evaluation of the relationship between silica flux particle size, reaction temperature and reaction time. This information could be combined with the temperature history of the particles and the frequency of collisions with iron oxides obtained from existing simulation techniques. The fayalite slag formation reaction in the reaction shaft could be predicted by this method, and the essential information could be obtained for completing the reaction of large silica fluxes within the shaft residence time. It could contribute to innovations in flash furnace technology in the copper smelting process.

CONCLUSIONS

In this study, to understand the fayalite slag formation reaction during a collision between iron oxide and silica flux in the reaction shaft of the flash furnace, the interfacial reaction behaviour between FeO powder and a large SiO_2 particle was directly observed by high-temperature microscopy. The FeO/SiO_2 significantly influences the rate of $FeO\text{-}SiO_2$ interfacial reaction because a liquid phase formed from low temperatures makes a new reaction interface and accelerates the reaction. The local FeO/SiO_2 in the reaction shaft must also be optimised to promote slag formation.

It is necessary to evaluate the effect of particle size, composition, and reaction temperature on the reaction rate in the future. These kinetic approaches may help to find the conditions under which the reaction can be completed, even with the large silica fluxes in the reaction shaft. It will contribute to future innovations in the copper smelting process using flash furnaces.

ACKNOWLEDGEMENTS

The authors are grateful to Mr Takashi Kamaya and Ms. Miho Hayasaka of Tohoku University, who operated the SEM-EDS system at the Institute of Multidisciplinary Research for Advanced Materials (IMRAM), as well as Mr. Hiroshi Takasuka of Sumitomo Metal Mining Co., Ltd., who operated the SEM-EDS system at the Sumitomo Metal Mining Co., Ltd.

REFERENCES

Ahokainen, T. and Jokilaakso, A., 1998. 'Numerical Simulation of the Outokumpu Flash Smelting Furnace Reaction Shaft', *Canadian Metallurgical Quarterly,* 37(3-4), 275-283.

Bale, C. W., Bélisle, E., Chartrand, P., Decterov, S. A., Eriksson, G., Hack, K., Jung, I. H., Kang, Y. B., Melançon, J., Pelton, A. D., Robelin, C. and Petersen, S., 2009. 'FactSage thermochemical software and databases — recent developments', *Calphad,* 33(2), 295-311.

COP28, 2023. 'COP28 delivers historic consensus in Dubai to accelerate climate action',

De Wilde, E., Bellemans, I., Campforts, M., Guo, M., Vanmeensel, K., Blanpain, B., Moelans, N. and Verbeken, K., 2016. 'Study of the Effect of Spinel Composition on Metallic Copper Losses in Slags', *Journal of Sustainable Metallurgy,* 3(2), 416-427.

Goto, Y., Kawanishi, S., Natsui, S., Takahashi, J.-i. and Nogami, H., 2024. 'In Situ Microscale Observation of FeOx–SiO2 Interfacial Reaction', *Metallurgical and Materials Transactions B*.

Hahn, Y. B. and Sohn, H. Y., 1990. 'Mathematical Modeling of Sulfide Flash Smelting Process: Part I. Model Development and Verification with Laboratory and Pilot Plant Measurements for Chalcopyrite Concentrate Smelting', *Metallurgical Transactions B,* 21B, 945-958.

ICSG, 2023. 'The World Copper Factbook 2023', [online], available: https://icsg.org/copper-factbook/ [Accessed December 14th 2023].

Jak, E., Hayes, P., Pelton, A. and Decterov, S., 2007. 'Thermodynamic optimisation of the FeO-Fe2O3-SiO2(Fe-O-Si) system with FactSage', *Int. J. Mat. Res.,* 98(9), 847-854.

Kemori, N., Denholm, W. T. and Kurokawa, H., 1989. 'Reaction Mechanism in a Copper Flash Smelting Furnace', *Metallurgical Transactions B,* 20B, 327-336.

Kojo, I. V., Jokilaakso, A. and Hanniala, P., 2000. 'Flash smelting and converting furnaces: A 50 year retrospect.', *JOM,* 52, 57-61.

Kojo, I. V., Reuter, M. A. and Scheidema, M. N., 2015. 'Primary Copper Smelting Impact', in *EMC*, 77-93.

Muan, A., 1955. 'Phase Equilibria in the System FeO-Fe2O3-SiO2', *Journal of Metals*, 965-976.

Natsui, S., Goto, Y., Takahashi, J.-i. and Nogami, H., 2023. 'Pattern analysis of the combustions of various copper concentrate tablets using high-speed microscopy and video-based deep learning', *Chemical Engineering Science,* 276, 118822.

Nirmal Kumar, S., Desai, B., Tathavadkar, V., Patel, Y., Patel, J., Singh, A., Vakil, K. and Kanakanand, S., 2022. 'CFD modelling of copper flash smelting furnace – reaction shaft', *Mineral Processing and Extractive Metallurgy,* 132(1), 49-61.

Nishioka, N., Tsurusaki, R., Hasegawa, S. and Takebe, H., 2022. *Direct observation of the copper concentrates ignition and combustion reaction with a lab-scale experiment,* translated by Santiago, Chile.

Shishin, D., Jak, E. and Decterov, S. A., 2018. 'Thermodynamic Assessment of Slag–Matte–Metal Equilibria in the Cu-Fe-O-S-Si System', *Journal of Phase Equilibria and Diffusion,* 39(5), 456-475.

Solnordal, C. B., Jorgensen, F. R. A., Koh, P. T. L. and Hunt, A., 2006. 'CFD modelling of the flow and reactions in the Olympic Dam flash furnace smelter reaction shaft', *Applied Mathematical Modelling,* 30(11), 1310-1325.

Takebe, H., Takahashi, Y. and Okura, T., 2019. 'Evaluation of Oxidation Reaction of Copper Concentrate Mixed with Silica Sand by Hot-Thermocouple Method', *Journal of Sustainable Metallurgy,* 5(2), 210-218.

Taskinen, P., Dinsdale, A. and Gisby, J., 2005. 'Industrial slag chemistry: A case study of computational thermodynamics', *Scandinavian Journal of Metallurgy,* 34(2), 100-107.

Taskinen, P. and Jokilaakso, A., 2021. 'Reaction Sequences in Flash Smelting and Converting Furnaces: An In-depth View', *Metallurgical and Materials Transactions B,* 52(5), 3524-3542.

Vartiainen, A., 1982. 'Schematic Presentation of Copper Losses within the Homogeneous Field of Fe-O-SiO2 Slags', *Scandinavian Journal of Metallurgy,* 11, 239-242.

White, M., Haywood, R., Ranasinghe, D. J. and Chen, S., 2015. *The development and application of a CFD model of copper flash smelting,* translated by CSIRO, Melbourne, Australia: 7-9.

Yazawa, A., 1979. 'Thermodynamic Evaluations of Extractive Metallurgical Processes', *Metallurgical Transactions B,* 10B, 307-321.